NACA RM L53F12

NACA

# RESEARCH MEMORANDUM

## THE CALCULATED AND EXPERIMENTAL INCREMENTAL LOADS AND MOMENTS PRODUCED BY SPLIT FLAPS OF VARIOUS SPANS AND SPANWISE LOCATIONS ON A 45° SWEPTBACK WING OF ASPECT RATIO 8

By H. Neale Kelly

Langley Aeronautical Laboratory
Langley Field, Va.





NATIONAL ADVISORY COMMITTEE
FOR AERONAUTICS

WASHINGTON

September 4, 1953

NATIONAL ADVISORY COMMITTEE FOR AERONAUTICS

RESEARCH MEMORANDUM

# THE CALCULATED AND EXPERIMENTAL INCREMENTAL LOADS AND MOMENTS PRODUCED BY SPLIT FLAPS OF VARIOUS SPANS AND SPANWISE LOCATIONS ON A 45° SWEPTBACK WING OF ASPECT RATIO 8

By H. Neale Kelly

## SUMMARY

The incremental lift and pitching moments produced by 20-percent-chord split flaps of various spans at various spanwise positions on two 45° sweptback wings of aspect ratio 8.02 have been obtained by pressure-distribution tests in the Langley 19-foot pressure tunnel. These data were obtained in the linear angle-of-attack range at a Reynolds number of 4,000,000 and a Mach number of 0.19.

The experimental data indicated that inboard flaps were far more effective in producing lift than outboard flaps (a 20-percent-span inboard flap produced approximately twice the increment in lift produced by a 40-percent-span outboard flap). Furthermore it was found that, in contrast to the case for straight wings, the flap lift effectiveness ($\alpha_\delta$) and the chordwise center of pressure of the incremental loads produced by full-span flaps on sweptback wings vary along the flap span.

Comparison with the experimental data indicated that the procedure of NACA Technical Note 2278 can be used to predict the integrated increments in lift and wing-root bending moment produced by flaps on high-aspect-ratio, highly sweptback wings with fair accuracy. Probable causes of the deviations of the calculated loadings from the experimental have been discussed.

For these wings the accuracy of the incremental pitching moment computed by the method outlined in NACA Wartime Report L-164 is dependent primarily upon the accurate prediction of the spanwise load distribution. The spanwise variation of the chordwise center of pressure of the load produced by the longer span flaps could, by a simple modification of the method, be closely approximated.

## INTRODUCTION

A knowledge of the magnitude of the effects of flap geometry and position on the span loading and pitching-moment characteristics of a wing is required in the aerodynamic and structural design of aircraft. Theoretical methods such as reference 1 are available for predicting the loading produced by a deflected flap on straight and swept wings and the semiempirical method of reference 2 is available for approximating the incremental twisting and pitching moments. Because of the lack of large-scale experimental data, the applicability of the methods of references 1 and 2 to wings with large amounts of sweep and relatively high aspect ratio, such as have been proposed for long-range, high-speed bombers, has not been ascertained.

A general low-speed investigation is being made in the Langley 19-foot pressure tunnel on two $45^{\circ}$ sweptback wings having aspect ratios of 8.02 and taper ratios of 0.45. One of the wings is untwisted and incorporates an NACA $63_1$A012 airfoil section in the free-stream direction; the other employs the same thickness distribution, but contains the calculated amount of twist and camber required to produce an elliptic span load distribution and a uniform chordwise distribution at a lift coefficient of 0.7 and a Mach number of 0.9.

As part of this investigation tests have been made, through the linear angle-of-attack range at a Reynolds number of 4,000,000 and a Mach number of 0.19, on the wings equipped with 20-percent-chord split flaps of various spans at various spanwise positions. Pressure data have been obtained in these tests at seven spanwise stations by means of orifices alined in the free-stream direction along the wing and flap surfaces.

The present paper contains the results of these tests and affords a comparison in a previously unchecked aspect-ratio—sweep range of the incremental lift and pitching moment calculated by the methods of references 1 and 2 with experimental data. Results of other phases of the general investigation may be found in references 3 to 8.

## SYMBOLS

$C_L$ wing lift coefficient, $\int_0^{1.0} c_l \frac{c}{\bar{c}} d\left(\frac{2y}{b}\right)$

$c_l$ section lift coefficient,

$$\cos(\alpha + \epsilon) \int_0^{1.0} \left(S_u - S_l\right) d\left(\frac{x}{c}\right) -$$

$$\sin(\alpha + \epsilon) \int_{(-z/c)_{max}}^{(z/c)_{max}} \left(S_r - S_f\right) d\left(\frac{z}{c}\right)$$

$C_b$ wing-root bending-moment coefficient,

$$\int_0^{1.0} \frac{c}{\bar{c}} \frac{2y}{b} \left[\cos \epsilon \int_0^{1.0} \left(S_u - S_l\right) d\left(\frac{x}{c}\right) - \sin \epsilon \int_{-(z/c)_{max}}^{(z/c)_{max}} \left(S_r - S_f\right) d\left(\frac{z}{c}\right)\right] d\left(\frac{2y}{b}\right)$$

$c_m$ section pitching-moment coefficient about $c/4$,

$$\int_0^{1.0} \left(S_u - S_l\right)\left(0.25 - \frac{x}{c}\right) d\left(\frac{x}{c}\right) + \int_{-(z/c)_{max}}^{(z/c)_{max}} \left(S_r - S_f\right) \frac{z}{c} d\left(\frac{z}{c}\right)$$

$C_m$ wing pitching-moment coefficient about $c'/4$,

$$\int_0^{1.0} c_{m_{c'/4}} \frac{c^2}{c'\bar{c}} d\left(\frac{2y}{b}\right)$$

$c_{m_{c'/4}}$ section pitching-moment coefficient about $c'/4$,

$$c_m + \frac{x_{c'/4}}{c} c_l$$

$a$ wing lift-curve slope, $\frac{dc_l}{d\alpha}$

| | |
|---|---|
| $b$ | wing span |
| $c$ | local chord parallel to plane of symmetry |
| $c'$ | mean aerodynamic chord, $\frac{2}{S_w}\int_0^{1.0} c^2 d\left(\frac{2y}{b}\right)$ |
| $\bar{c}$ | mean geometric chord, $\frac{S_w}{b}$ |
| $S$ | pressure coefficient, $\frac{H - p}{q}$ |
| $H$ | free-stream total pressure |
| $p$ | local static pressure |
| $q$ | free-stream dynamic pressure, $\frac{1}{2}\rho V^2$ |
| $\alpha_\delta$ | flap lift effectiveness, $\frac{dc_l}{d\delta}\Big/\frac{dc_l}{d\alpha}$ |
| $\rho$ | density of air |
| $V$ | free-stream velocity |
| $S_w$ | wing area |
| $x$ | longitudinal distance from local leading edge measured parallel to chord plane and plane of symmetry |
| $x_{cp}$ | center of pressure of loading produced by flaps, fraction of local chord |
| $x_{c'/4}$ | longitudinal distance from $c'/4$ to $c/4$ |
| $y$ | lateral distance from plane of symmetry measured perpendicular to plane of symmetry |
| $z$ | vertical distance from chord plane measured perpendicular to chord plane |
| $\alpha$ | angle of attack of root chord |
| $\epsilon$ | geometric angle of twist of any section referred to the root chord (negative if washout) |

$\Delta$ increment produced by flaps

$\delta$ flap deflection angle measured in a plane parallel to the plane of symmetry

Subscripts:

u upper surface

l lower surface

f forward of maximum thickness

r rearward of maximum thickness

## MODEL AND TESTS

Experimental data presented in the present paper were obtained from tests of two wings of similar plan form. Each wing had an aspect ratio of 8.02, a taper ratio of 0.45, and 45° sweepback of the quarter-chord line. One wing was untwisted and embodied NACA $63_1$A012 airfoil sections in the free-stream direction; the other, which employed the amount of camber and twist determined by the method of reference 9 required to produce an elliptic span load distribution and a uniform chordwise load distribution at a lift coefficient of 0.7 and a Mach number of 0.9, utilized the same thickness distribution about a modified $a = 1.0$ mean line. The untwisted, symmetrical wing and the 80-percent-chord line (twist reference axis) of the twisted and cambered wing had no dihedral. Additional geometric information can be obtained from figure 1 and references 3 and 4.

Both wings consisted of a solid steel core to which a bismuth-tin alloy was bonded. Surface orifices, distributed as illustrated in figure 2 (wing orifices are listed in refs. 4 and 7) were provided for measuring the pressures on the left half-wing. Tubes, leading from the orifices, embedded in the bismuth-tin alloy were brought out through the 20-percent-semispan station of the right half-wing. These tubes were conducted through a fairing (as shown in figs. 2 and 3) to multitube manometers.

Flaps used in the present investigation were of the split type and were 20 percent of the local wing chord measured parallel to the plane of symmetry. The flaps were constructed of sheet steel with provisions made for measuring pressures (see fig. 2 for locations) and were attached by means of steel angle block to the under surface of the wings. Flaps on the twisted and cambered wing were deflected 11.3° relative to the

local wing-chord plane while those on the untwisted, symmetrical wing were deflected 52.2° relative to the lower surface of the wing.

Full-span flaps, 60-percent-span inboard flaps, 40-percent-span outboard flaps, and 20-percent-span flaps at various spanwise locations were tested on the twisted and cambered wing. A 60-percent-span flap was tested on the untwisted, symmetrical wing.

Pressure data were obtained through an angle-of-attack range from -2.6° to 4.8° for the twisted and cambered wing and from 0.6° to 9.0° for the untwisted symmetrical wing.

All tests reported herein were conducted on smooth models in the Langley 19-foot pressure tunnel at a tunnel pressure of approximately $2\frac{1}{3}$ atmospheres. The Reynolds number, based on the mean aerodynamic chord, and the corresponding Mach number of the tests were $4.0 \times 10^6$ and 0.19, respectively.

## REDUCTION AND CORRECTION OF DATA

Section lift and pitching-moment data were obtained by numerical integration of the chordwise pressure distributions.

All data in the present report have been corrected for jet-boundary interference and airstream-angle variation in the region occupied by the models. More detailed discussions of these corrections may be found in references 4 and 7. No corrections were applied to take into account the spanwise variation of the jet-boundary-induced angle or the model twist due to air load.

For all calculations on the twisted and cambered wing involving the flap deflection, a modified flap deflection was used. This modified flap deflection took into account the use of a flat flap on the highly cambered lower surface of the wing and was effectively the flap deflection relative to the lower surface of the wing. This modified flap deflection was determined by the use of Glauert's thin-airfoil theory and its variation along the span is presented in figure 2.

## REVIEW OF ANALYTICAL METHODS

### Incremental Spanwise Loading

Any of the existing methods for calculating the spanwise loading for swept wings could be utilized to calculate the incremental loading produced

by a partial-span flap provided sufficient spanwise control points were used in the solution to describe accurately the abrupt changes in the loading encountered at the end of the flap. The large number of control points required would, however, complicate the mathematical solution and necessitate the expenditure of an excessive amount of computing time. An alternate procedure which makes possible the use of a small number of control points in the solution is presented in reference 1.

In order to utilize a solution involving few control points in the calculation of the incremental loading produced by flaps, the discontinuous twist distribution produced by such flaps must be approximated by a fictitious twist distribution which will yield the correct loading at these control points. Since this fictitious twist distribution is assumed to be independent of plan-form effects the relatively simple, exact solution for partial-span flaps on the zero-aspect-ratio wing (ref. 10) can be utilized in its calculation. Using the procedure outlined in reference 1, for any given method for calculating the spanwise loading on straight and swept wings, a fictitious twist distribution can be developed that will permit the calculation of the incremental loading produced by flaps without the use of an excessive number of control points in the solution.

Reference 1 uses the twist distribution determined for the zero-aspect-ratio wing in the procedure of reference 11 which is based on the simplified Weissinger 7-control-point solution of Prandtl's lifting surface theory to calculate the loading at four spanwise positions across the semispan ($2y/b = 0$, 0.383, 0.707, and 0.904). A special interpolation formula is also provided for the interpolation of the loading at four intermediate positions ($2y/b = 0.195$, 0.556, 0.831, and 0.981). For fractional wing-chord flaps the full wing-chord flap loading obtained by this procedure is modified by the use of the two-dimensional flap lift effectiveness for the flap chord and deflection used.

## Incremental Pitching Moment

According to reference 2, the center of pressure of the incremental lift load produced by flaps over the flapped part of a wing $x_{cp_f}$ (relative to the leading edge) can be determined with satisfactory accuracy by the relation $x_{cp_{f_1}} = \frac{a_o}{a}\left(x_{cp_{f_o}} - 0.25\right) + 0.25$ in which $a$ is the lift-curve slope and the subscript $o$ pertains to the two-dimensional airfoil. The center of pressure over the unflapped portion is then approximated by a line faired between the 0.40-chord station at the flap end to the 0.25-chord station at a point 30 percent of the semispan from the flap

end; the center of pressure is thereafter assumed to fall along the 0.25-chord line as illustrated in the following sketch:

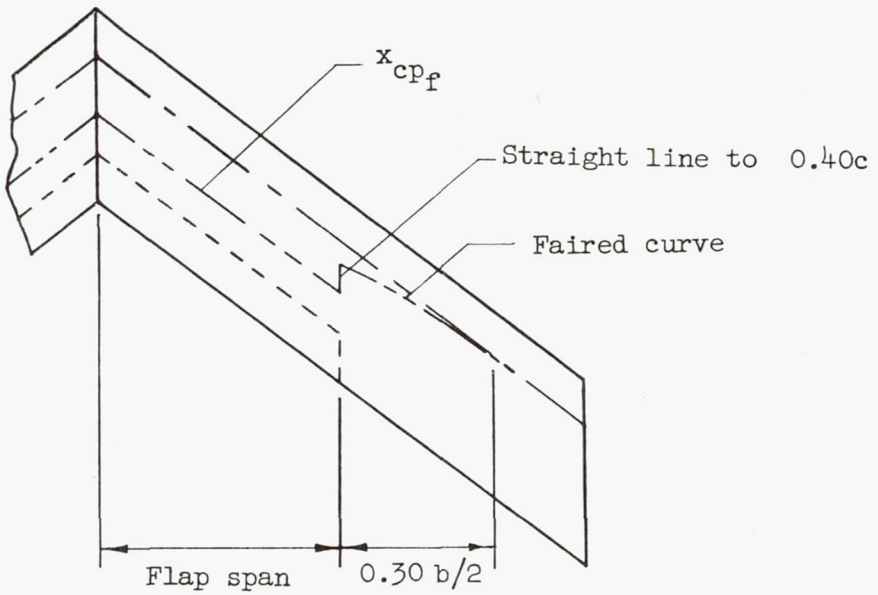


The variation of the chordwise center of pressure thus determined is then used in conjunction with the moment arm produced by sweepback and spanwise position and the incremental loading produced by flaps to determine the incremental pitching moment.

## RESULTS AND DISCUSSION

Since most of the data refer to the twisted and cambered wing all remarks in the following discussion, unless specified otherwise, will pertain to the twisted and cambered wing.

### Basic Data

The section lift and pitching-moment characteristics for the various flap configurations are presented in figure 4. These characteristics have been obtained by numerical integration of chordwise pressure-distribution measurements and are plotted against the root section angle of attack.

In general, the section lift and pitching-moment coefficients presented in figure 4 vary linearly with root section angle of attack; however, at the outer spanwise stations, as the negative lift range is

approached, there is a strong positive trend of the local pitching moment for all configurations tested. Examination of the pressure distributions seems to indicate that this positive trend is due to flow separation over the lower surface induced by the large negative angles of attack at which the section is operating (see twist distribution, fig. 1).

In contrast to the flap lift effectiveness $\alpha_\delta$ for straight wings, which is for all practical purposes the same at all spanwise positions as that determined two dimensionally (as illustrated by the experimental data presented in ref. 12) the lift effectiveness for full-span flaps on the present sweptback wing varies considerably along the flap span. In order to illustrate this difference more clearly, the spanwise variations of $\alpha_\delta$ for full-span flaps on a straight wing and the sweptback wing have been presented in figure 5.

## Spanwise Loading

The calculated incremental span loadings produced by deflected flaps presented in figure 6 were obtained by the method of reference 1. Also included in the figure are the incremental loadings obtained by using the method of reference 1 in conjunction with the 15-control-point Weissinger solution which provides for the calculation of the loading at eight spanwise positions across the semispan ($2y/b$ = 0, 0.195, 0.383, 0.556, 0.707, 0.831, 0.924, and 0.981).

The values of flap lift effectiveness $\alpha_\delta$ obtained from reference 1, intended primarily for plain flaps of small deflection, were not considered adequate for the flaps used in the present investigation. The values of 0.35 and 0.19 used as the flap lift effectiveness for the twisted and cambered, and plane wing sections, respectively, in the calculated loadings presented in the present paper were, therefore, estimated from two-dimensional data.

The experimental incremental loadings presented in figure 6 have been obtained from the basic data presented in figure 4. The experimental spanwise loadings have been faired so as to integrate to approximately the same increment in lift as measured in force tests.

It is apparent from figure 6 that the shapes of the loadings calculated by means of reference 1 for the shorter span flaps show poor agreement with the experimentally determined loadings. Examination reveals that this distortion of the calculated loadings occurs primarily at the points where the loading is interpolated. This would indicate that, due to the small number of control points used, the interpolation formula of reference 1 cannot accurately predict the abrupt loading changes induced by short-span flaps.

Further comparison of the loadings in figure 6 reveals a tendency of the method of reference 1 to underpredict the incremental loading produced by flaps over the inboard part of the wing and overpredict the loading over the outboard part. In reference 5 a similar tendency of the Weissinger solution to underpredict the unflapped wing loading over the inboard part of the wing and overpredict the loading over the outboard part was virtually eliminated by using 15 control points in the solution instead of 7.

As might be expected, use of the Weissinger 15-control-point solution in the method of reference 1 greatly improves the shapes of the incremental loadings produced by the shorter span flaps. Although the use of 15 control points improves the agreement between the calculated and experimental loadings, the tendency of the calculated loadings to underpredict the loading over the inboard part of the wing and overpredict the loading over the outboard part remains. This tendency is due at least in part to the use of a constant, two-dimensional flap lift effectiveness across the wing span. Experimentally it is found that the lift effectiveness varies considerably across the span as shown in figure 5.

Examination of the method of reference 1 in the light of the material contained in reference 5 would indicate that the method of reference 1 should exhibit an over-all underprediction of incremental load produced by flaps on the present wings. This underprediction would increase with increased flap deflection and would be similar to the underprediction of the unflapped wing lift-curve slope found in reference 5. In general this appears to be true. To illustrate this trend, the calculated and experimental span loadings due to a 60-percent-span, 52.2° deflected flap on the untwisted, symmetrical wing are presented in figure 7. The modified loading, which exhibits better agreement with the experimental loading, was obtained by multiplying the originally predicted loading by the ratio of the experimental to the calculated lift-curve slope $\frac{0.069}{0.062}$.

The variations with flap span and position of the incremental lift and root-bending-moment coefficient due to deflected flaps as obtained by mechanical integration of the experimental loadings and the loadings calculated by means of reference 1 are presented in figure 8. It is shown by the experimental curve in figure 8 that the inboard flaps are far more effective in producing lift than outboard flaps. (A flap extending 20 percent of the semispan out from the plane of symmetry produces approximately twice the increment in lift produced by a flap extending 40 percent of the semispan in from the tip.) The increase in the constant-span or unit-flap lift producing ability as the flap is moved inboard is, as shown by the experimental curve, large enough to overcompensate for the decrease in moment arm of the inboard flaps resulting in larger wing root-bending moments for the inboard flaps.

Although figure 8 graphically illustrates the underprediction of the incremental lift due to inboard flaps, the overprediction of the lift due to outboard flaps, and the resulting deviations of the root-bending moment from the experimental, it would appear, from the figure, that the method of reference 1 predicts the effects of span and position of flaps on high-aspect-ratio, highly sweptback wings with fair accuracy.

## Pitching Moment

The spanwise variations of the chordwise center of pressure of the loading produced by 60-percent-span flaps on the untwisted, symmetrical wing as determined experimentally and as calculated using the procedure of reference 2 (see section entitled "Review of Analytical Methods") are presented in figure 9(a). Both the calculated distribution based on the experimental lift-curve slope and the distribution based on the lift-curve slope calculated by the 7-control-point Weissinger solution essentially predict the experimental variations of the center of pressure. It is also apparent that on highly sweptback, high-aspect-ratio wings the accuracy of the method of reference 2 is far more dependent upon the accurate prediction of the spanwise distribution of the incremental load produced by flaps than the accurate prediction of the chordwise center of pressure.

While the calculated spanwise distribution of the incremental wing pitching moment produced by flaps based on the experimental lift-curve slope and loading closely approximates the experimental distribution (fig. 9(b)), the distribution based on the theoretical lift-curve slope and the calculated loading of reference 1 departs considerably from the experimental. (This is due primarily to the underprediction of the incremental loading discussed in the preceding section.) Although the incremental pitching moment of -0.0132 obtained by numerical integration of the pitching-moment distribution based on the theoretical lift-curve slope and loading compares favorably with the incremental pitching moments of -0.0042 for the experimental and -0.0156 for the calculated based on the experimental lift-curve slope and loading, in view of the distortion of the pitching-moment distribution (fig. 9(b)), it appears that this agreement is somewhat fortuitous. Nevertheless, it is believed that the use of the loading calculated by means of reference 1 in the method of reference 2 will yield a more accurate estimation of the incremental pitching moment produced by flaps on sweptback wings than the use of the straight-wing loading calculated by the method suggested in reference 2 or the use of this loading modified by simple sweep theory as suggested in reference 13.

The data presented in figure 10 indicate that in general the method of reference 2 does not predict the spanwise variation of the chordwise center of pressure of the incremental flap load with sufficient accuracy

for the prediction of the local section pitching or twisting moment. This lack of agreement of the experimental center of pressure and that calculated by the method of reference 2 is probably due to the spanwise variation of the section lift-curve slopes. (According to ref. 2 the equation for determining the center of pressure of the incremental load produced by flaps should give the best results when the local lift-curve slopes are equal to that of the wing as a whole.) In an attempt to improve the agreement, the method of reference 2 has been modified by utilizing the local lift-curve slope as determined experimentally in place of the wing lift-curve slope. This modification, as shown in figure 10, brings the experimental and calculated centers of pressure into close agreement at the root and improves the agreement across the flap. With the exception of the 20-percent-span flaps, the modification of reference 2 using the local lift-curve slope calculated by the Weissinger 7-control-point solution (also presented in fig. 10), although suffering a constant displacement of 0.05 of the local wing chord, closely approximates the experimental spanwise variation of chordwise center of pressure of the incremental load.

## CONCLUSIONS

The calculated and experimental incremental loads and moments produced in the linear angle-of-attack range by 20-percent-chord split flaps of various spans at various spanwise positions on two 45° sweptback wings of aspect ratio 8.02 have been obtained at a Reynolds number of 4,000,000 and a Mach number of 0.19 and the following results are indicated:

1. Inboard flaps are far more effective in producing lift than outboard flaps. (A flap which extends 20 percent of the semispan out from the plane of symmetry, although containing approximately the same area as a flap extending 40 percent of the semispan in from the tip, produces twice as much lift as the outboard flap.)

2. In contrast to the case of straight wings, the flap lift effectiveness ($\alpha_\delta$) and the chordwise center of pressure of the incremental loads produced by full-span flaps on sweptback wings vary along the flap span.

3. The procedure of NACA Technical Note 2278 predicts the integrated increments in lift and wing-root bending moment produced by flaps with fair accuracy. Deviations of the calculated incremental loadings from the experimental loadings can be attributed to inherent weaknesses of the 7-control-point Weissinger solution and the inability of the procedure to take into account the spanwise variation of the flap lift effectiveness ($\alpha_\delta$) found experimentally. The use of 15 control points in the solution tends to improve the agreement between the calculated and experimental loadings.

4. The accuracy of the method for computing the incremental pitching moment due to flaps presented in NACA Wartime Report L-164 is, in the high-aspect-ratio—sweep range, dependent primarily upon the accurate prediction of the spanwise load distribution. The method presented in that report could with slight modification be used to predict a spanwise variation of the chordwise center of pressure that, although suffering a constant displacement of 0.05 of the local wing chord, closely approximates the spanwise variation found experimentally for the larger flap spans.

Langley Aeronautical Laboratory,
National Advisory Committee for Aeronautics,
Langley Field, Va., May 27, 1953.

## REFERENCES

1. DeYoung, John: Theoretical Symmetric Span Loading Due to Flap Deflection for Wings of Arbitrary Plan Form at Subsonic Speeds. NACA TN 2278, 1951.

2. Pitkin, Marvin, and Maggin, Bernard: Analysis of Factors Affecting Net Lift Increment Attainable With Trailing-Edge Split Flaps on Tailless Airplanes. NACA WR L-164, 1944. (Formerly NACA ARR L4I18.)

3. Salmi, Reino J.: Low-Speed Longitudinal Aerodynamic Characteristics of a Twisted and Cambered Wing of 45° Sweepback and Aspect Ratio 8 With and Without High-Lift and Stall-Control Devices and a Fuselage at Reynolds Numbers From $1.5 \times 10^6$ to $4.8 \times 10^6$. NACA RM L52C11, 1952.

4. Graham, Robert R.: Low-Speed Characteristics of a 45° Sweptback Wing of Aspect Ratio 8 From Pressure Distributions and Force Tests at Reynolds Numbers from 1,500,000 to 4,800,000. NACA RM L51H13, 1951.

5. Schneider, William C.: A Comparison of the Spanwise Loading Calculated by Various Methods With Experimental Loadings Obtained on a 45° Sweptback Wing of Aspect Ratio 8 at a Reynolds Number of $4.0 \times 10^6$. NACA RM L51G30, 1952.

6. Pratt, George L., and Shields, E. Rousseau: Low-Speed Longitudinal Characteristics of a 45° Sweptback Wing of Aspect Ratio 8 With High-Lift and Stall-Control Devices at Reynolds Numbers From 1,500,000 to 4,800,000. NACA RM L51J04, 1952.

7. Pratt, George L.: Effects of Twist and Camber on the Low-Speed Longitudinal Stability Characteristics of a 45° Sweptback Wing of Aspect Ratio 8 at Reynolds Numbers From $1.5 \times 10^6$ to $4.8 \times 10^6$ As Determined by Pressure Distributions, Force Tests, and Calculations. NACA RM L52J03a, 1952.

8. Salmi, Reino J., and Jacques, William A.: Effect of Vertical Location of a Horizontal Tail on the Static Longitudinal Stability Characteristics of a 45° Sweptback-Wing—Fuselage Combination of Aspect Ratio 8 at a Reynolds Number of $4.0 \times 10^6$. NACA RM L51J08, 1952.

9. Cohen, Doris: A Method for Determining the Camber and Twist of a Surface To Support a Given Distribution of Lift, With Applications to the Load Over a Sweptback Wing. NACA Rep. 826, 1945. (Supersedes NACA TN 855.)

10. DeYoung, John: Spanwise Loadings for Wings and Control Surfaces of Low Aspect Ratio. NACA TN 2011, 1950.

11. DeYoung, John, and Harper, Charles W.: Theoretical Symmetric Span Loading at Subsonic Speeds for Wings Having Arbitrary Plan Form. NACA Rep. 921, 1948.

12. Sivells, James C., and Westrick, Gertrude C.: Method for Calculating Lift Distribution for Unswept Wings With Flaps or Ailerons by Use of Nonlinear Section Lift Data. NACA Rep. 1090, 1952. (Supersedes NACA TN 2283.)

13. Lowry, John G., and Schneiter, Leslie E.: Estimation of Effectiveness of Flap-Type Controls on Sweptback Wings. NACA TN 1674, 1948.

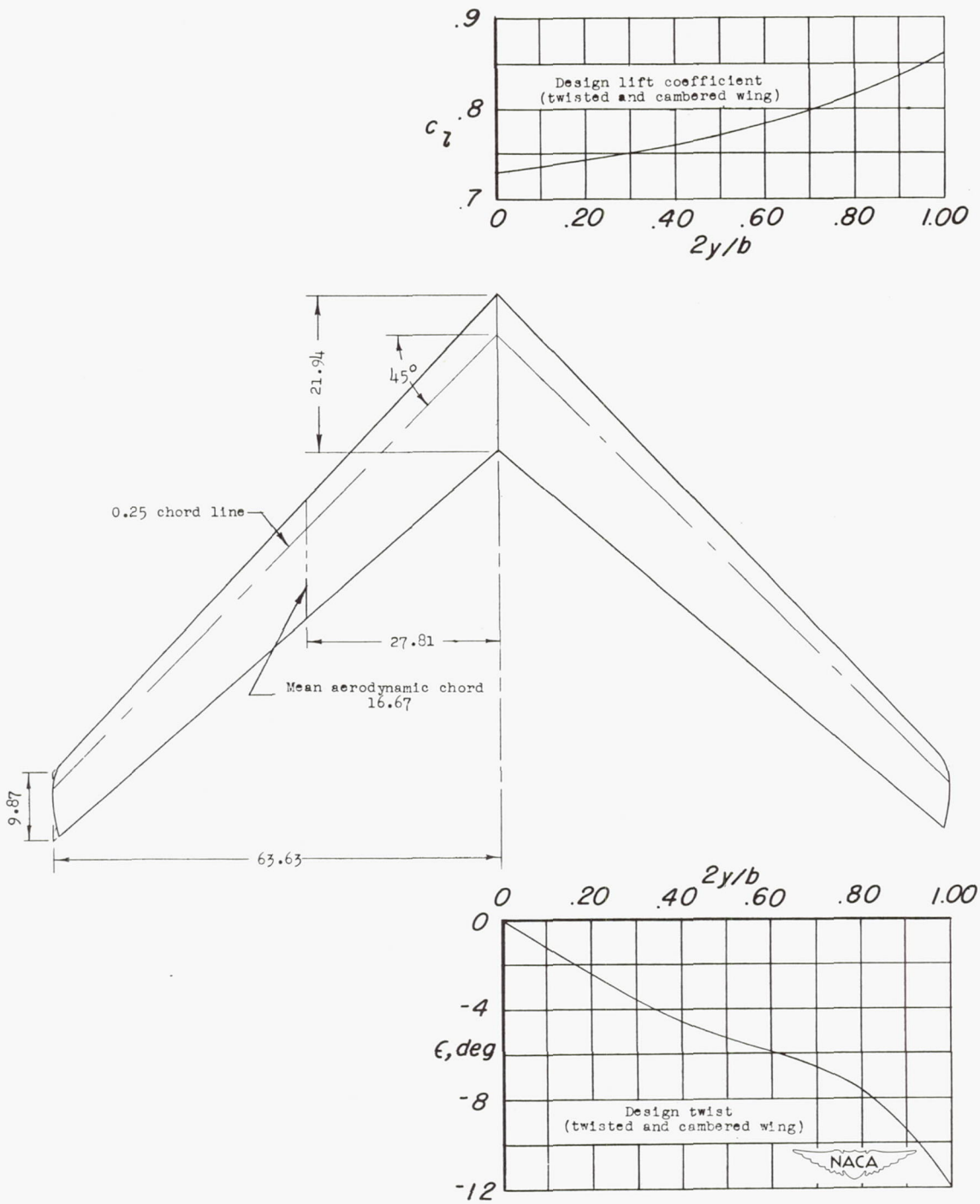


Figure 1.- Geometric characteristics of wings. Sweepback 45°, taper ratio 0.45, aspect ratio 8.02, area 14.02 square feet, NACA $63_1$A012 thickness distribution used throughout. (Dimensions in inches except as noted.)

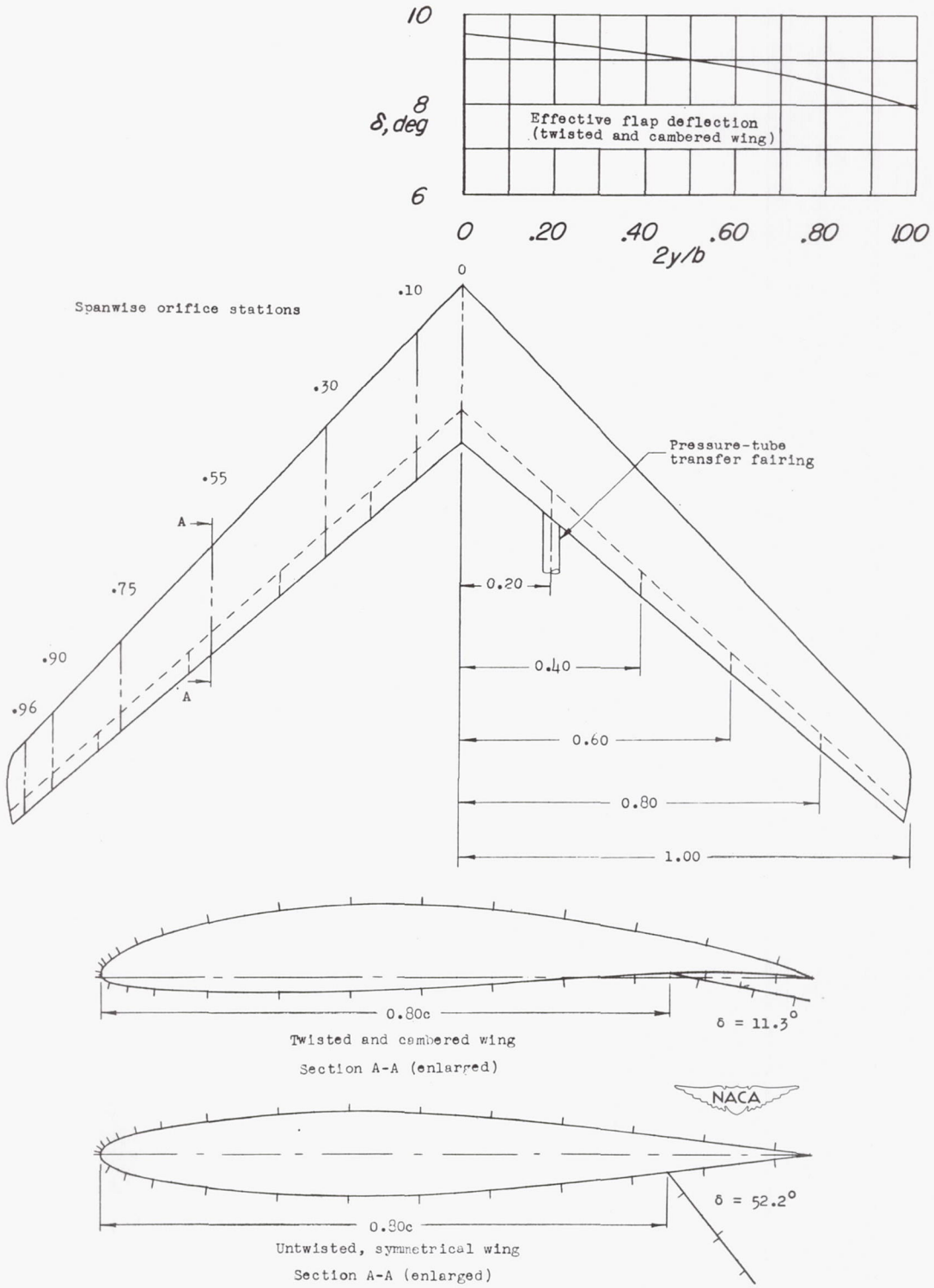


Figure 2.- Location of flaps and pressure orifices. (Dimensions in fractions of semispan except as noted.)

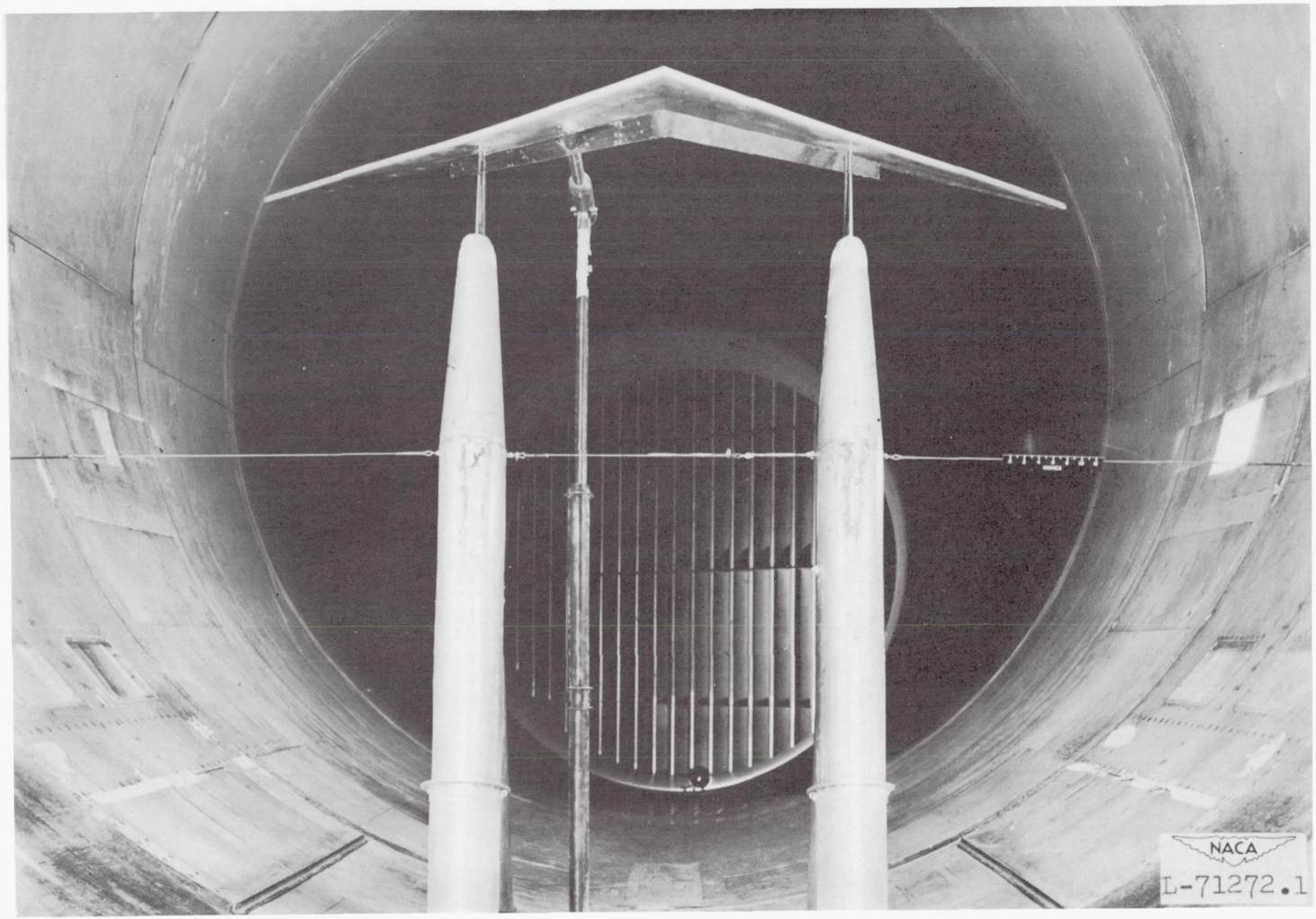


Figure 3.- Twisted and cambered wing equipped with 60-percent-span split flaps as mounted in the Langley 19-foot pressure tunnel for pressure-distribution tests.

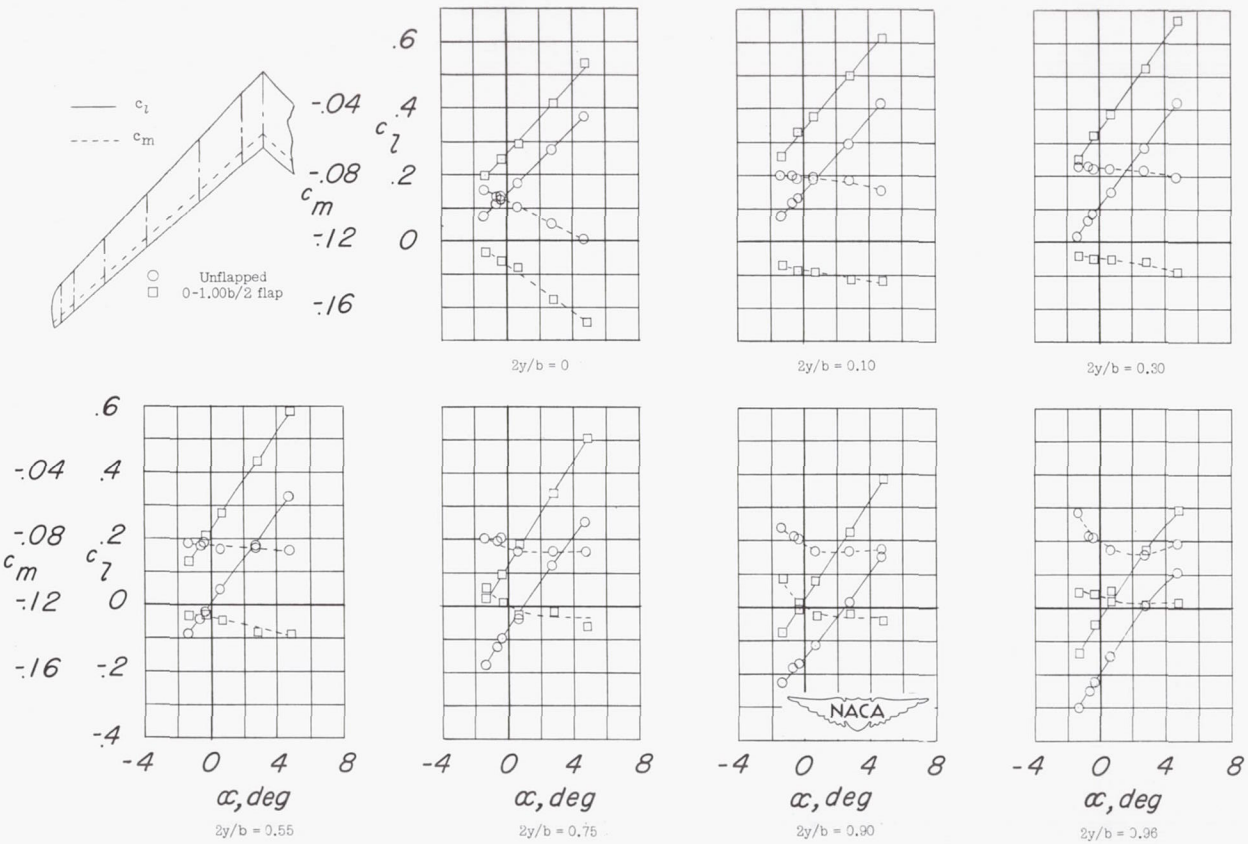


(a) Twisted and cambered wing, 0-1.00b/2 flap, $\delta = 11.3^{\circ}$.

Figure 4.- Variation with root section angle of attack of the local lift and pitching-moment coefficients with and without 0.20-chord split flaps.

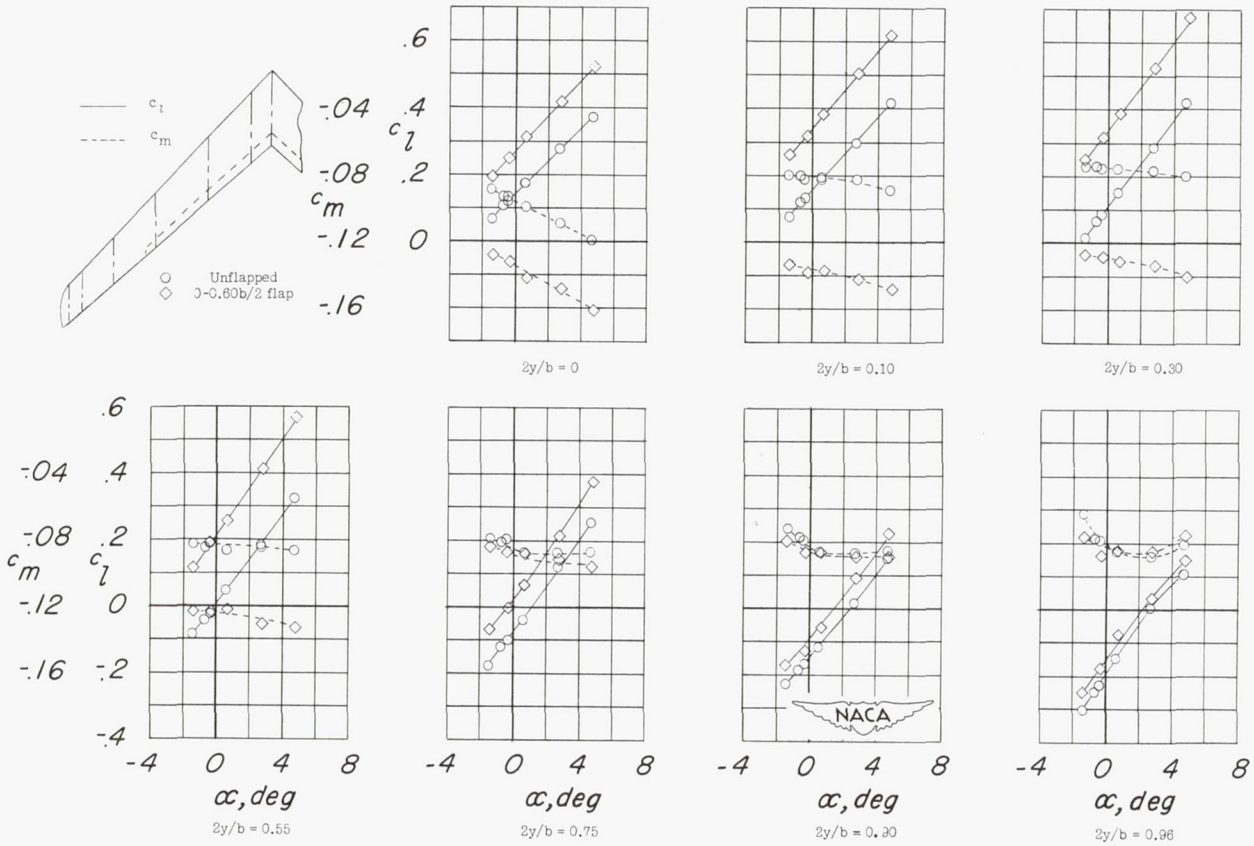


(b) Twisted and cambered wing, 0-0.60b/2 flap, $\delta = 11.3^{\circ}$.

Figure 4.- Continued.

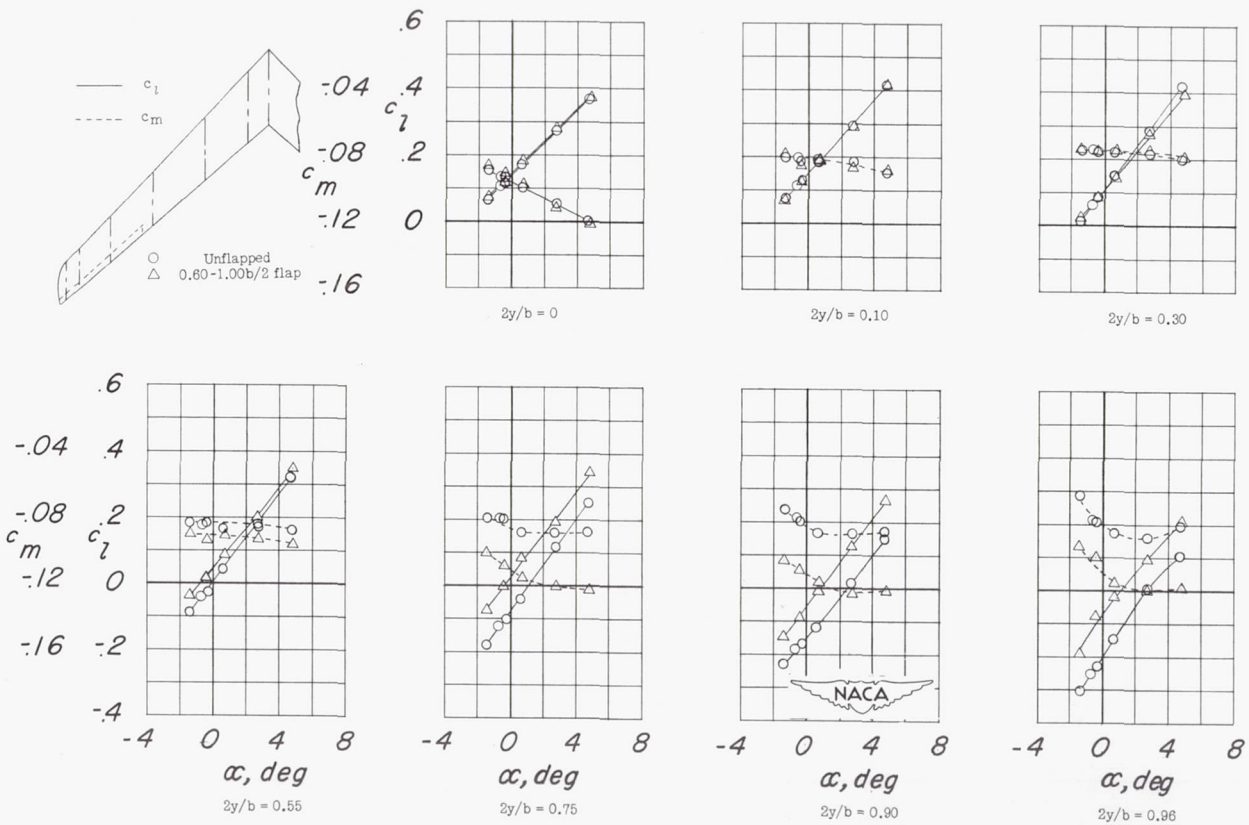


(c) Twisted and cambered wing, 0.60-1.00b/2 flap, $\delta = 11.3^{\circ}$.

Figure 4.- Continued.

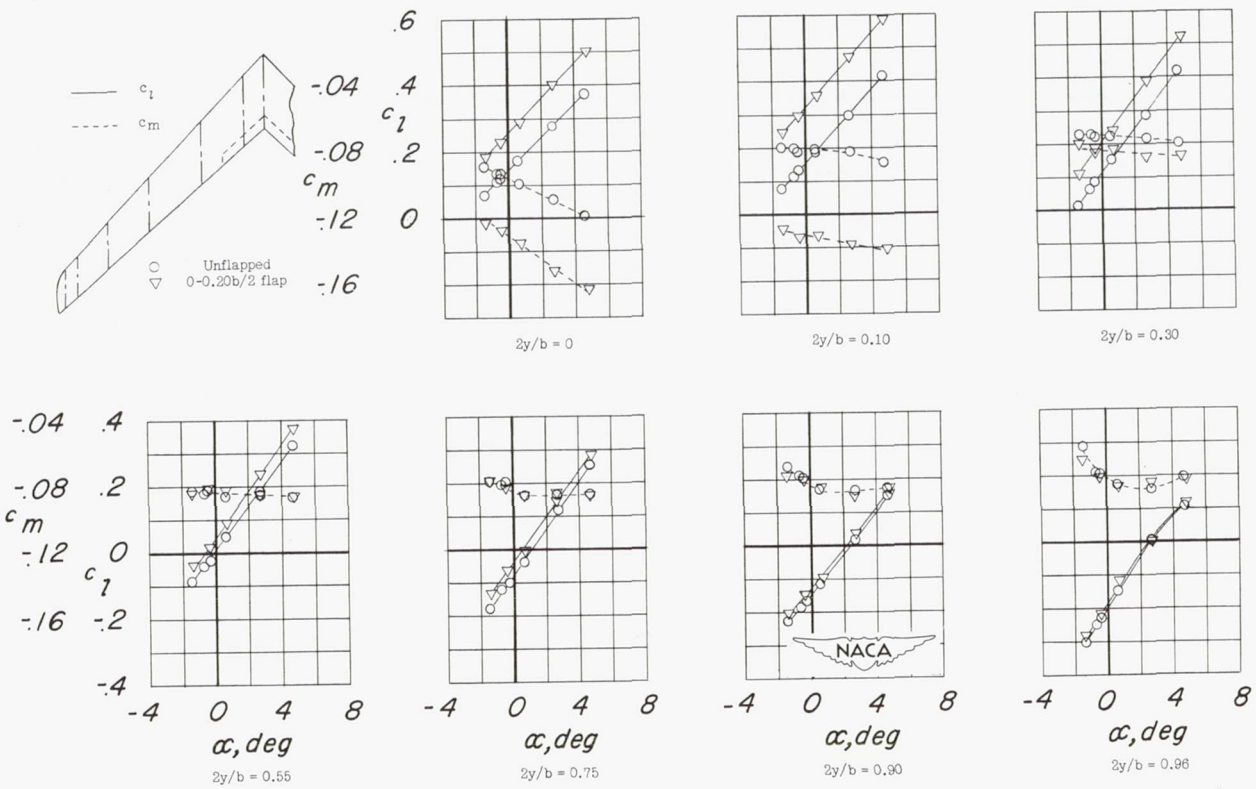


(d) Twisted and cambered wing, 0-0.20b/2 flap, $\delta = 11.3^{\circ}$.

Figure 4.- Continued.

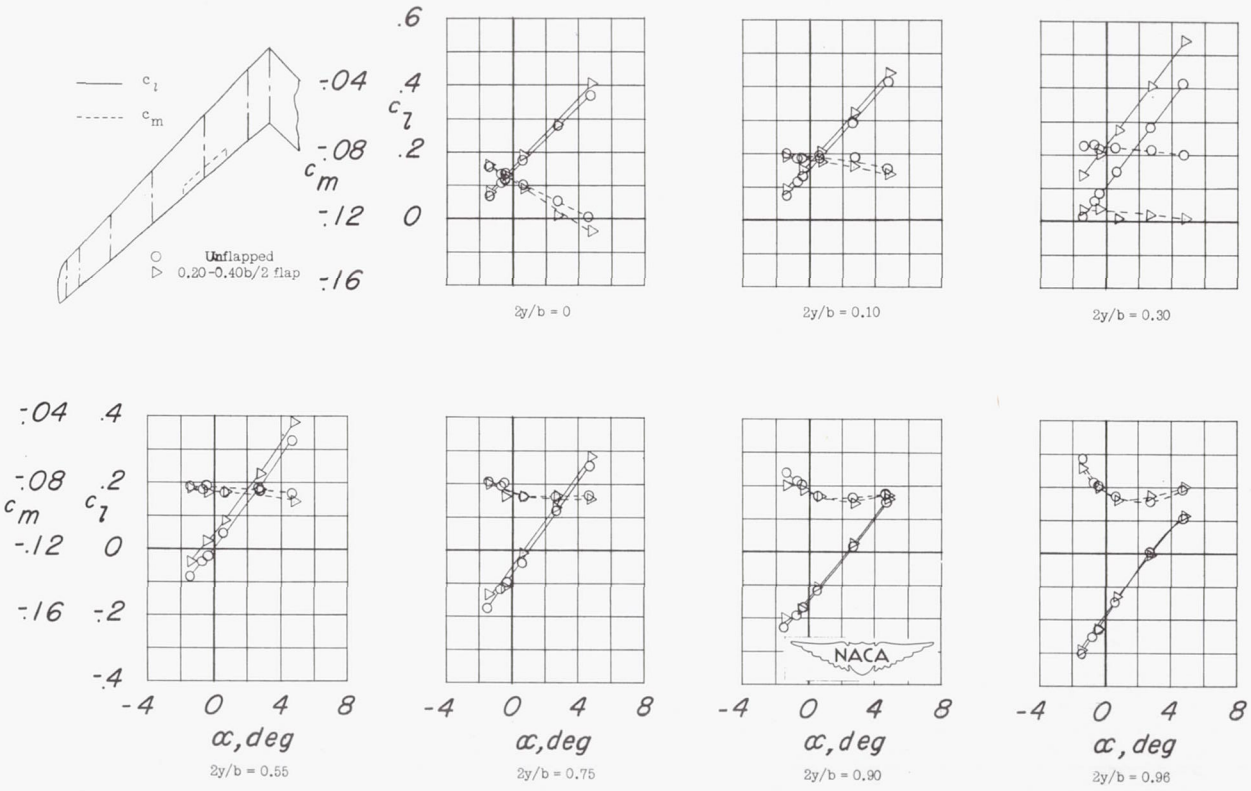


(e) Twisted and cambered wing, 0.20-40b/2 flap, $\delta = 11.3^{\circ}$.

Figure 4.- Continued.

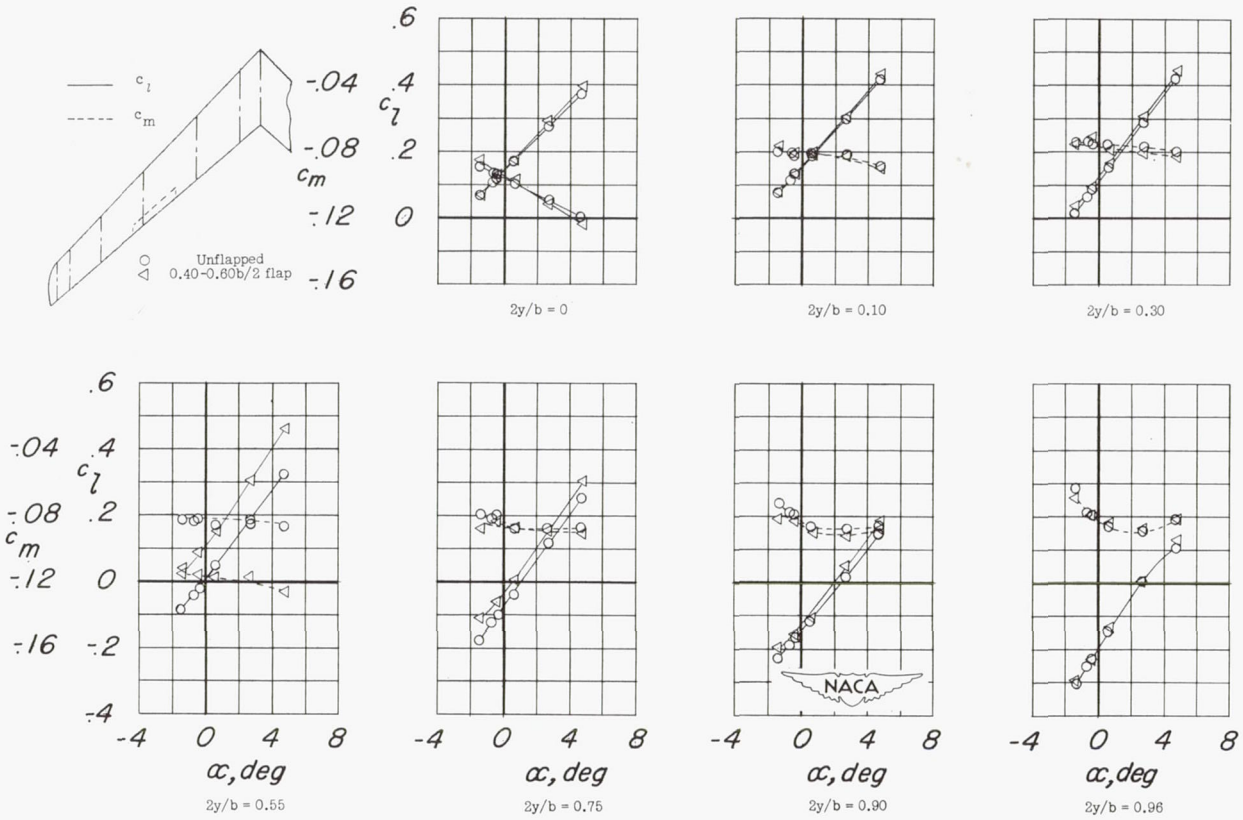


(f) Twisted and cambered wing, 0.40-0.60b/2 flap, $\delta = 11.3^{\circ}$.

Figure 4.- Continued.

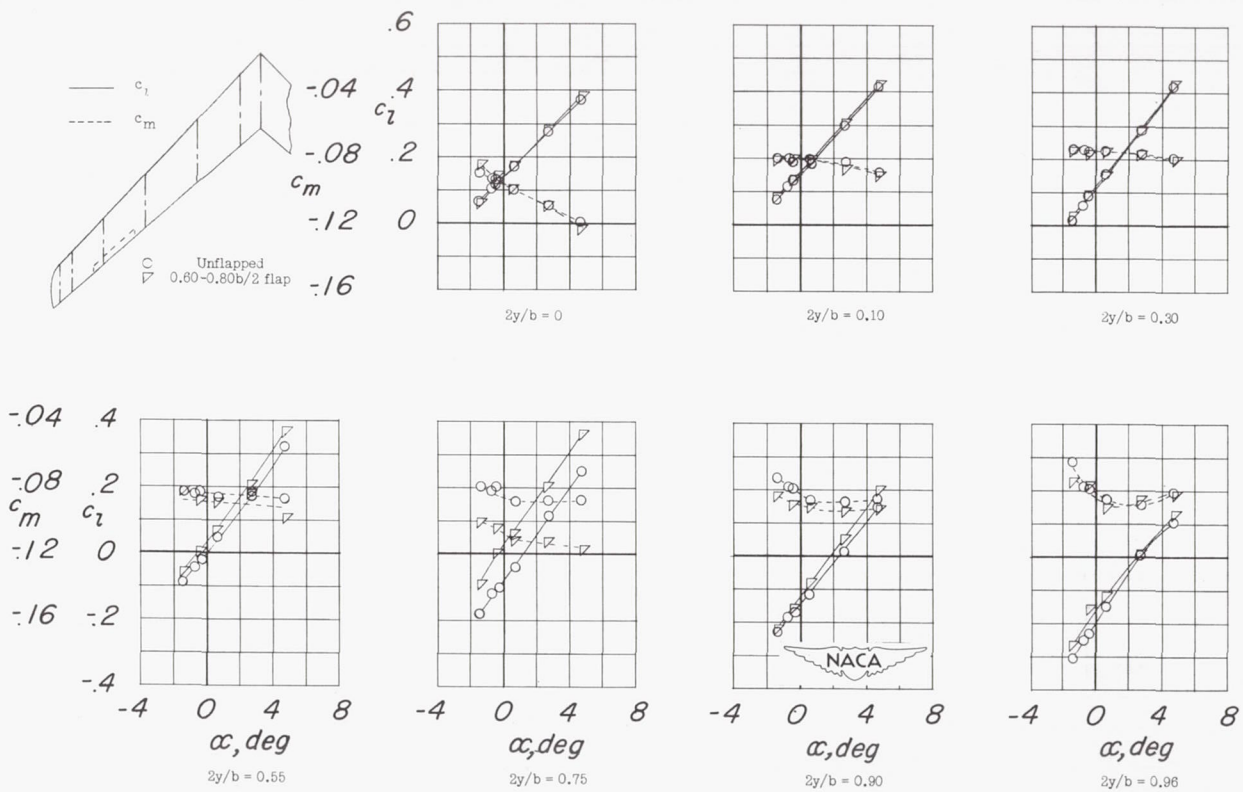


(g) Twisted and cambered wing, 0.60-0.80b/2 flap, $\delta = 11.3^\circ$.

Figure 4.- Continued.

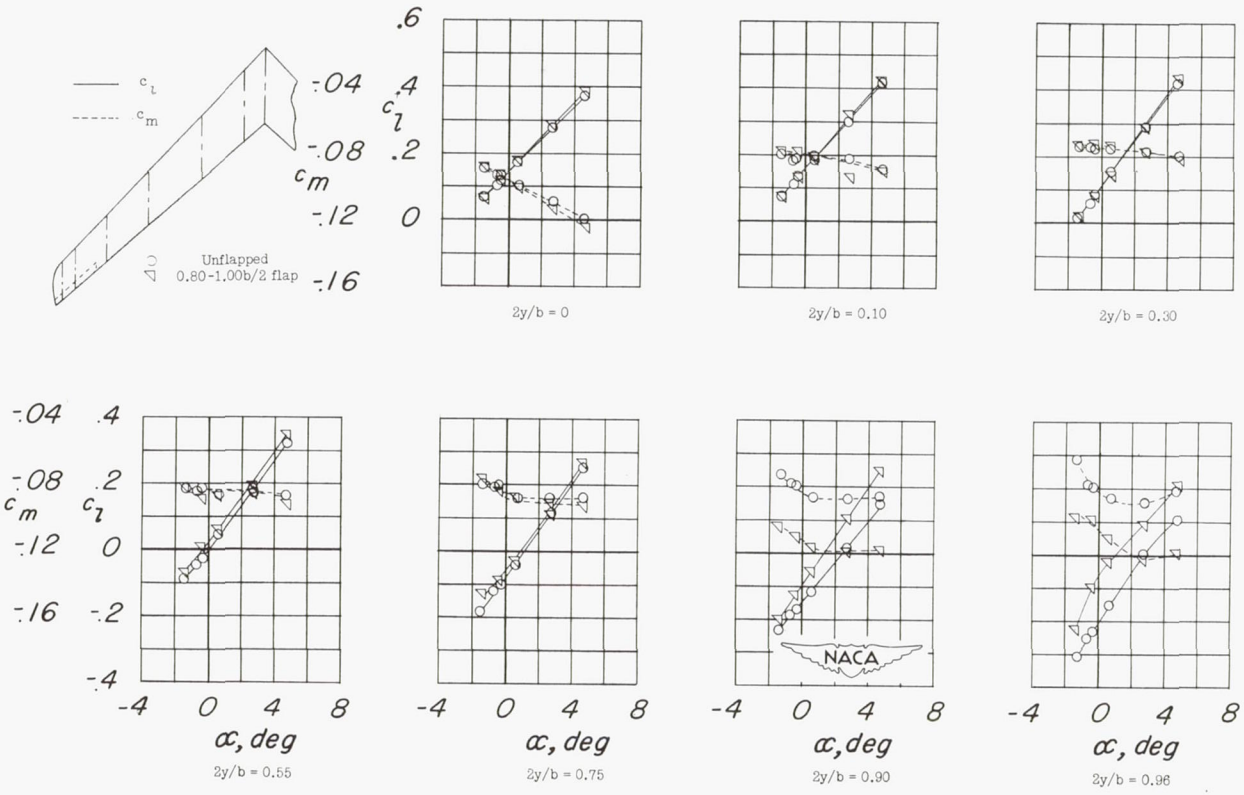


(h) Twisted and cambered wing, 0.80-1.00b/2 flap, $\delta = 11.3^{\circ}$.

Figure 4.- Continued.

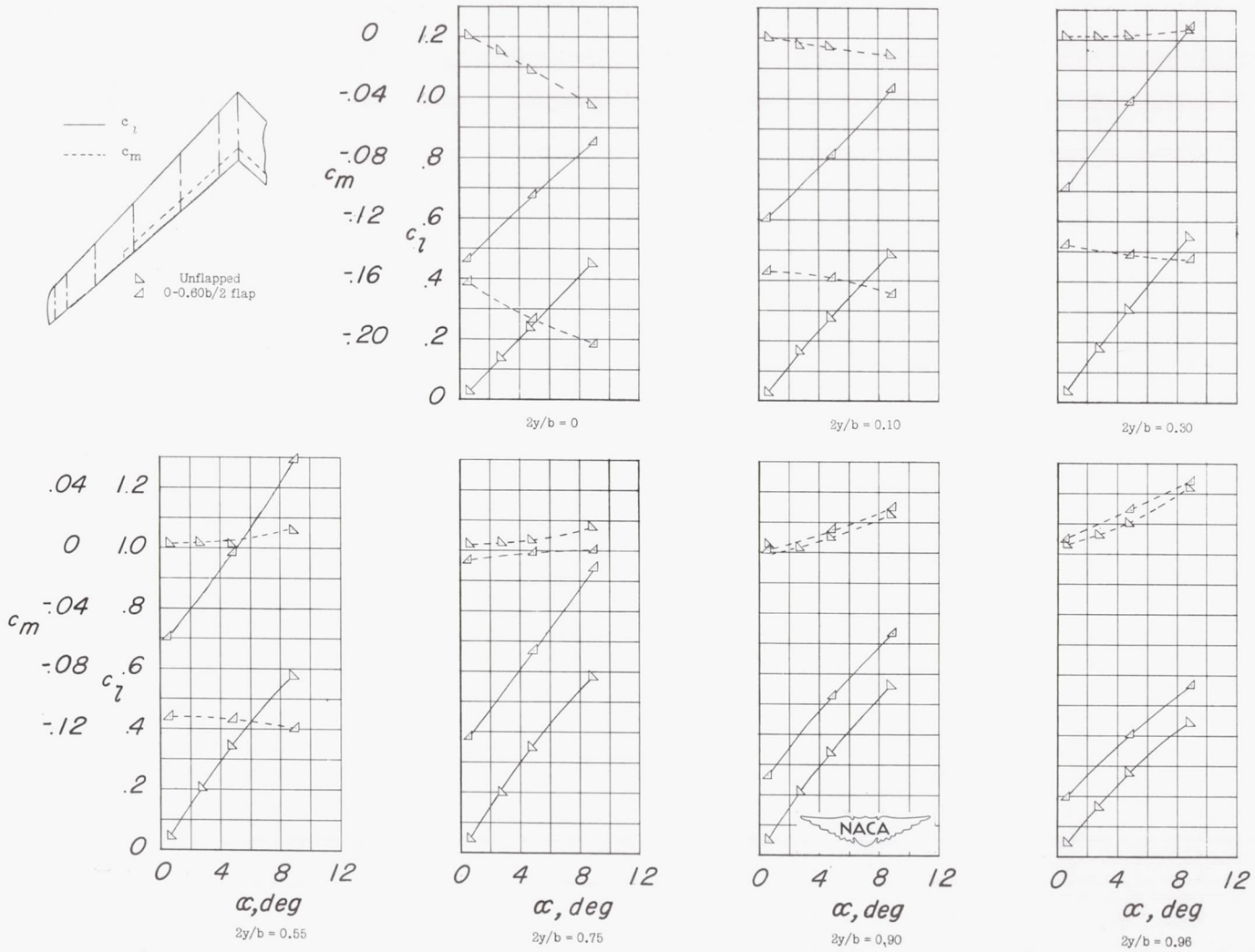


(i) Untwisted-symmetrical wing, 0-0.60b/2 flap, $\delta = 52.2^{\circ}$.

Figure 4.- Concluded.

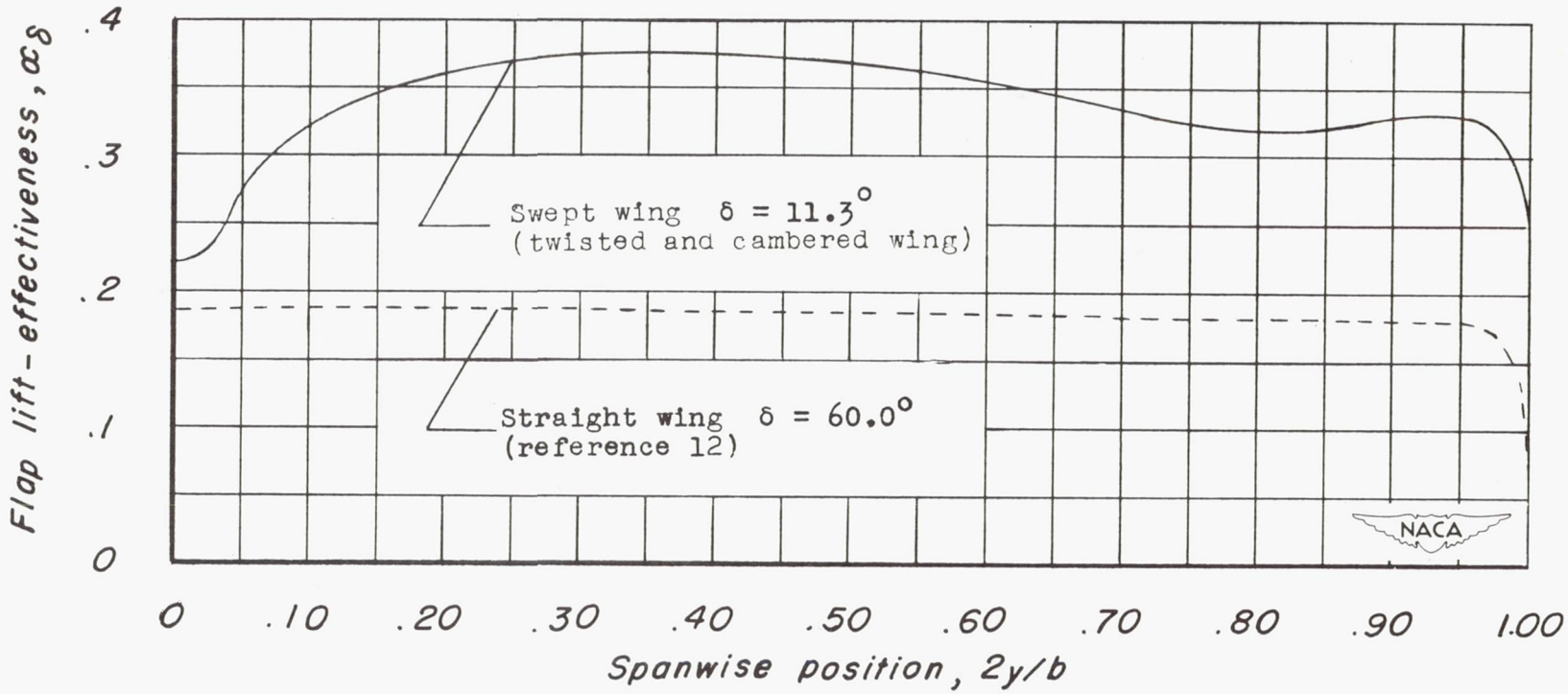


Figure 5.- A comparison of the spanwise variation of the flap lift effectiveness for full-span flaps on straight and swept wings.

RESTRICTED

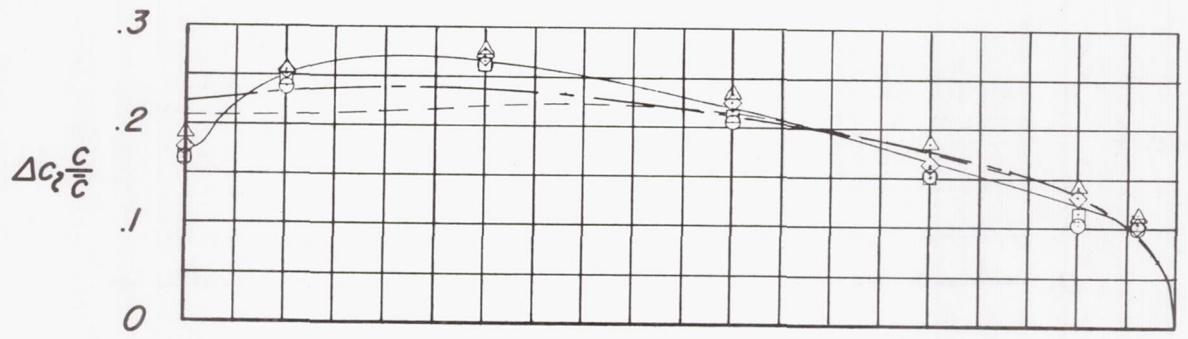


(a) 0-1.00b/2 flap.

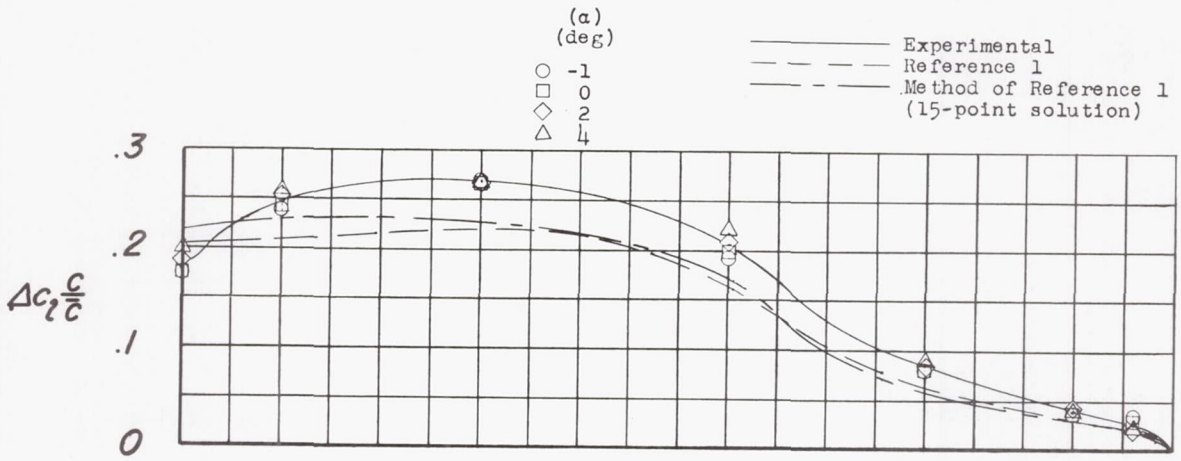


(b) 0-0.60b/2 flap.

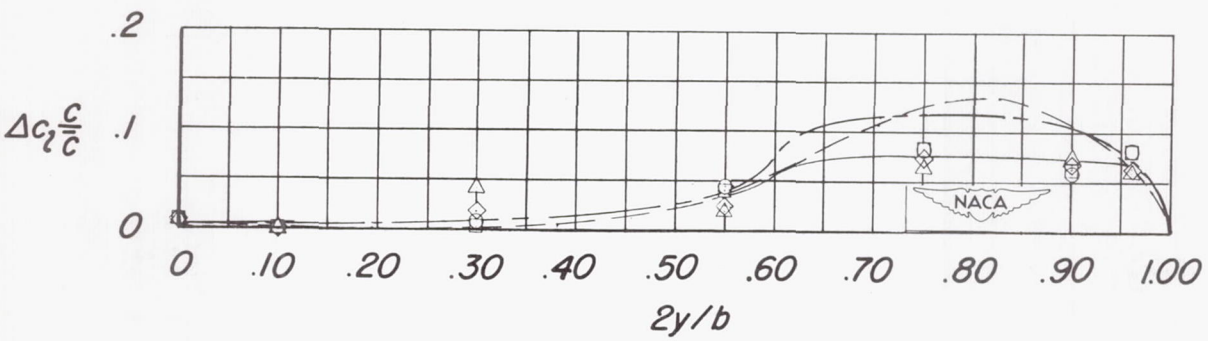


(c) 0.60-1.00b/2 flap.

Figure 6.- Calculated and experimental incremental span load distribution produced by 0.20-chord split flaps of various spans on the twisted and cambered wing. $\delta = 11.3^{\circ}$.

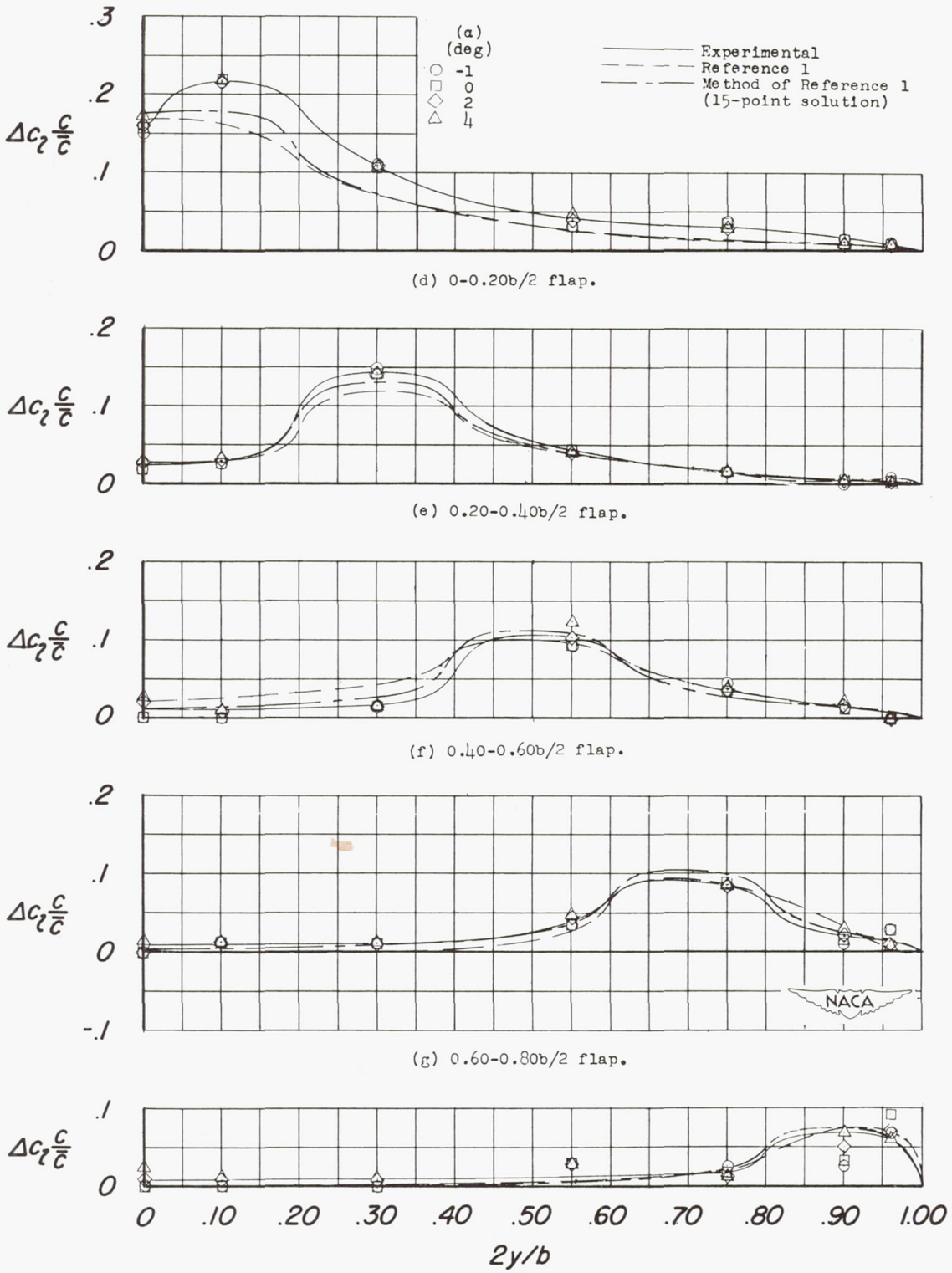


Figure 6.- Concluded.

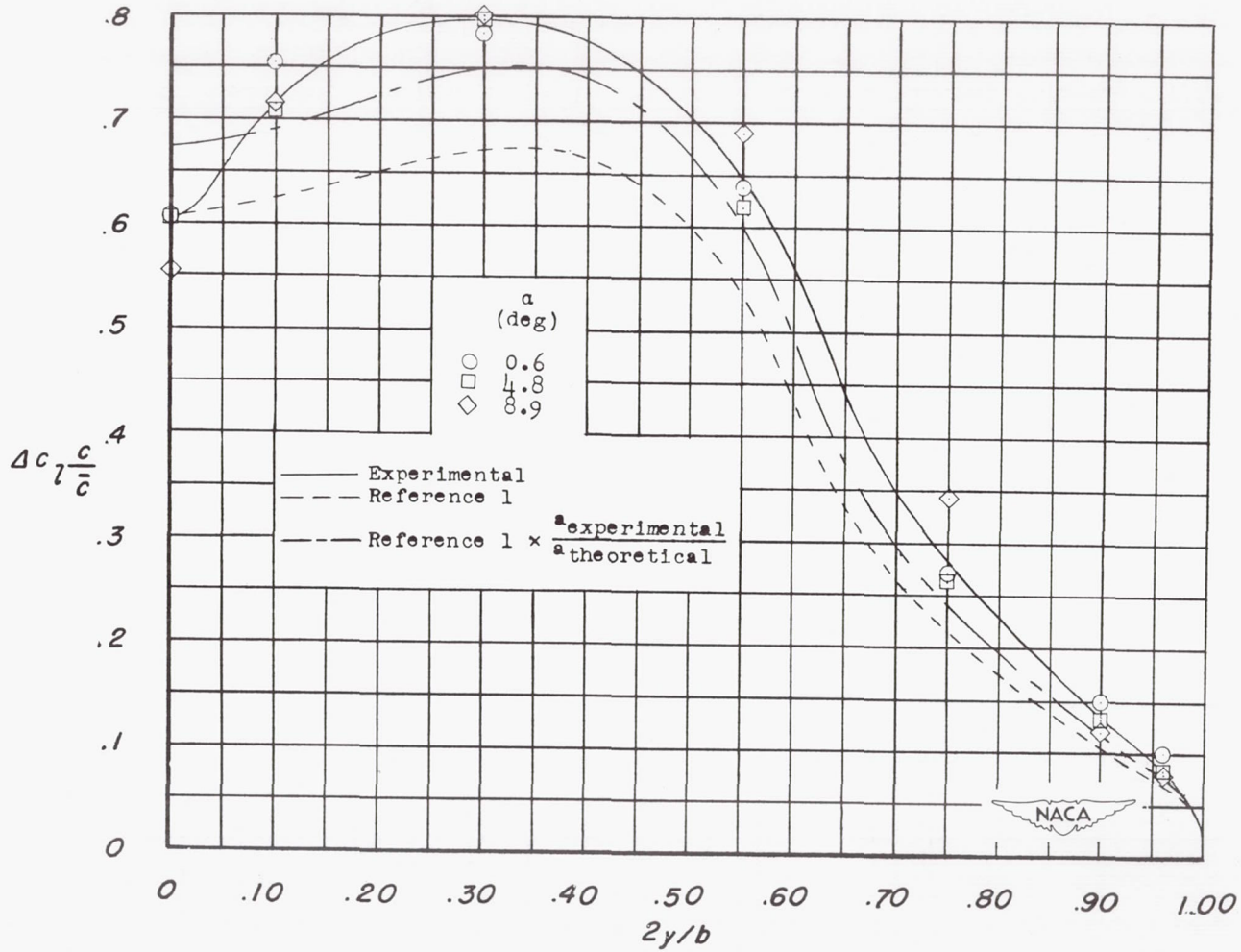


Figure 7.- Calculated and experimental incremental span load distribution produced by a 0.20-chord. 60-percent-span split flap on the untwisted, symmetrical wing. $\delta = 52.2^{\circ}$.

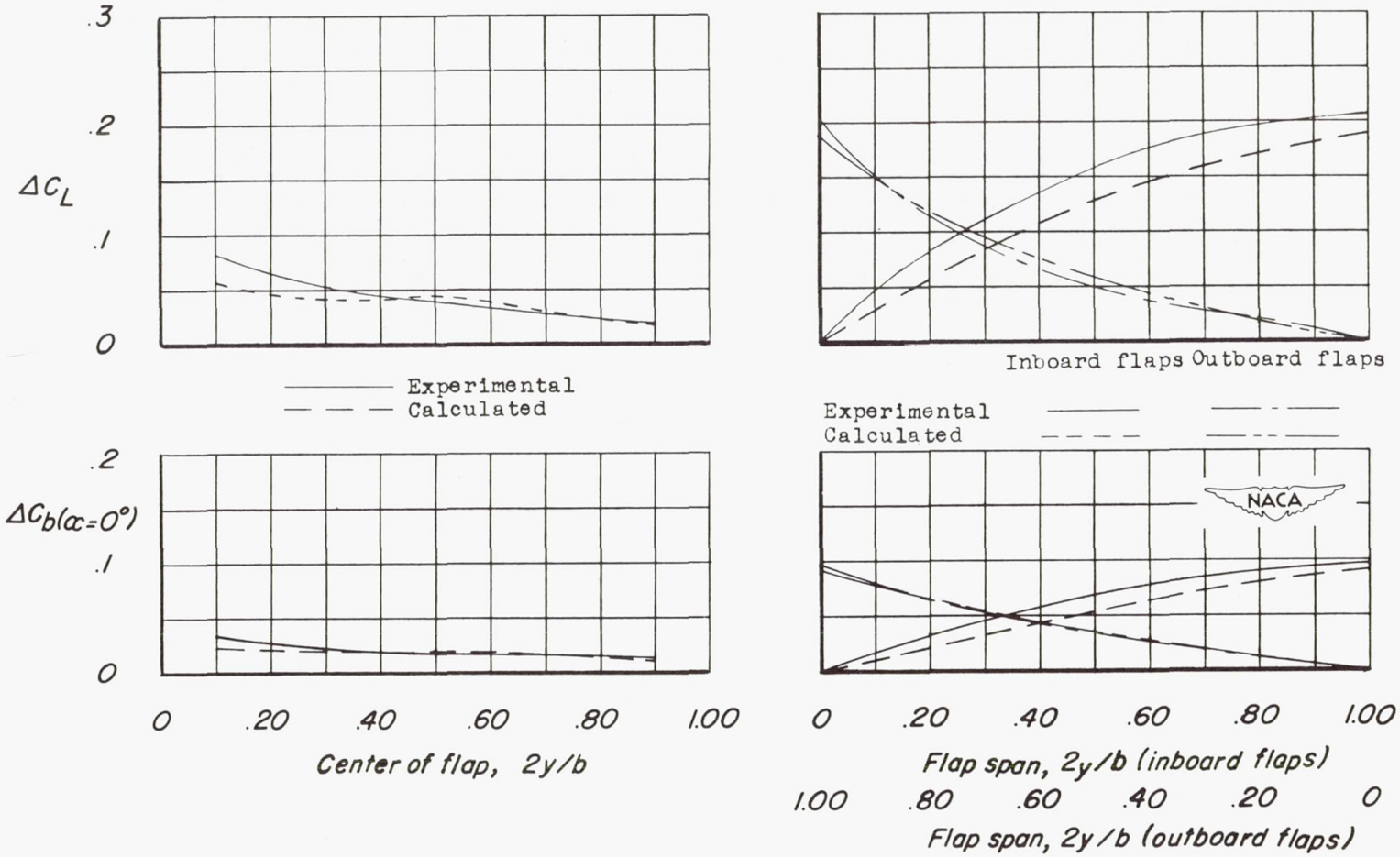


(a) Effect of flap position. (0.20b/2 flap)

(b) Effect of flap span.

Figure 8.- Variation with flap span and position of the incremental lift and wing root bending moment produced by flaps on the twisted and cambered wing. $\delta = 11.3°$.

B

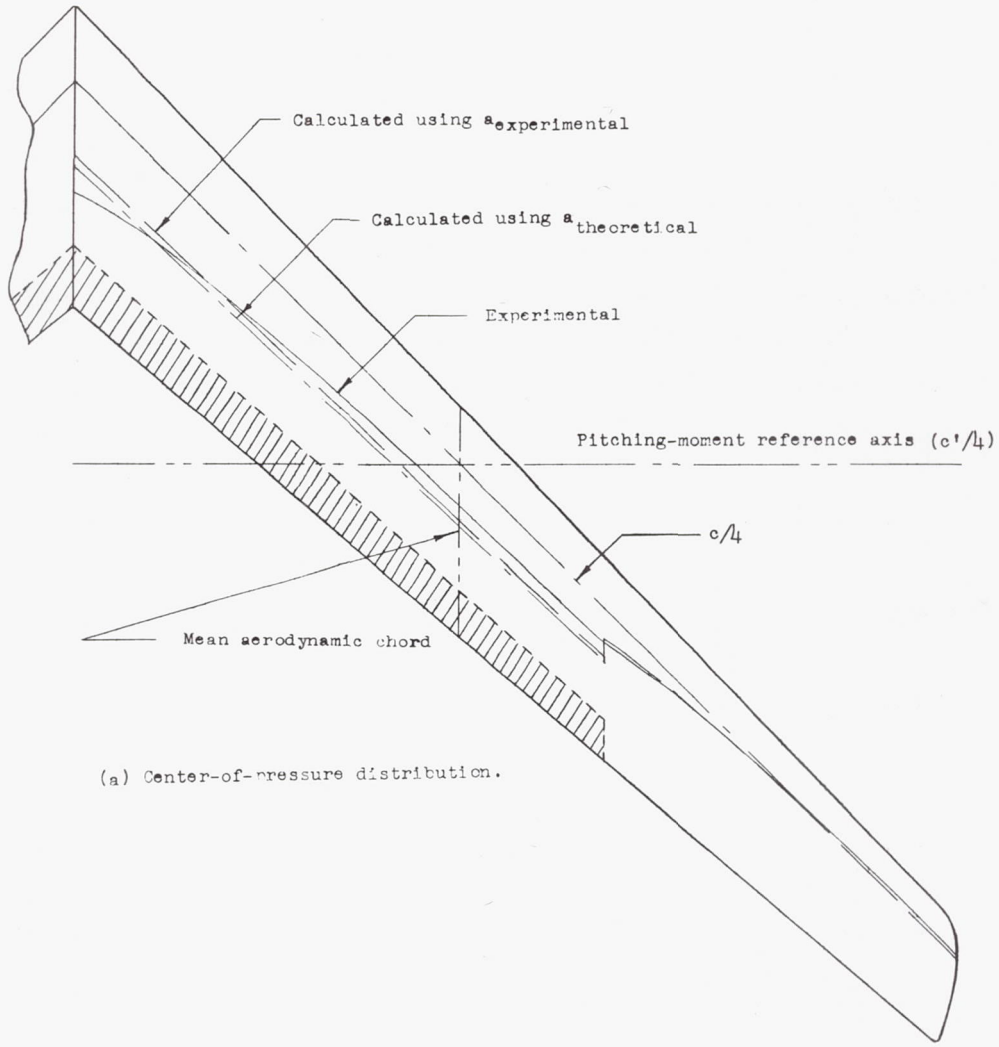


(a) Center-of-pressure distribution.

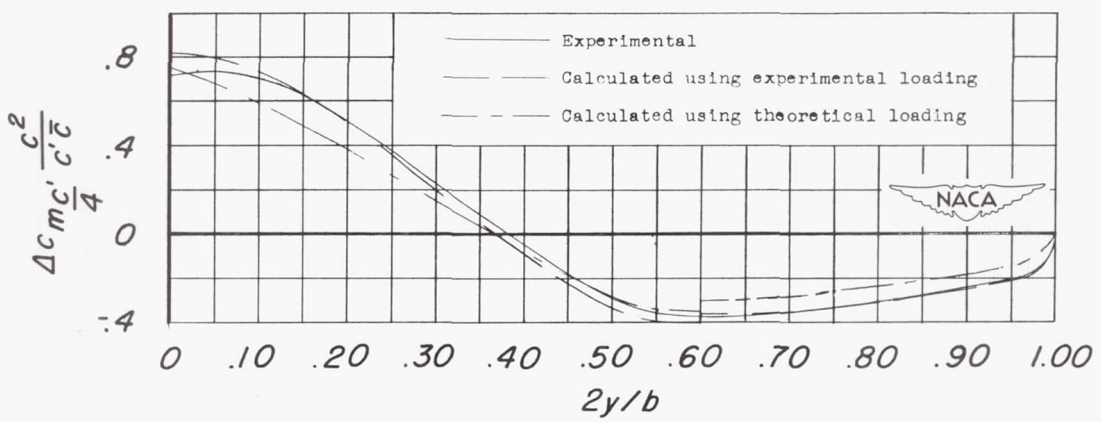


(b) Pitching-moment distribution.

Figure 9.- Calculated and experimental center-of-pressure and incremental-pitching-moment distribution produced by a 60-percent-span split flap on the untwisted, symmetrical wing. $\delta = 52.2^{\circ}$.

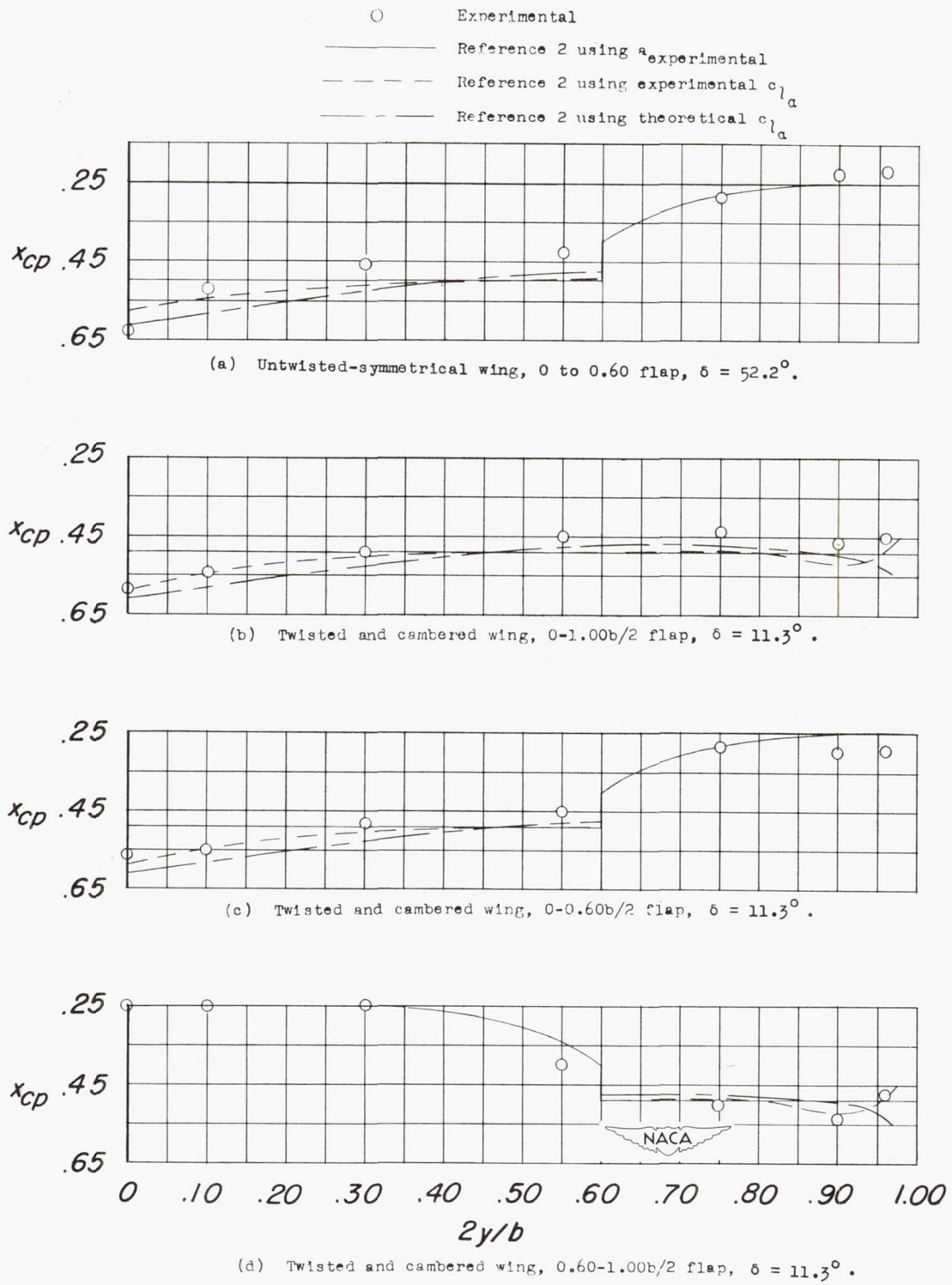


Figure 10.- Calculated and experimental spanwise variations of the center of pressure of the incremental loading produced by 0.20-chord flaps of various spans.

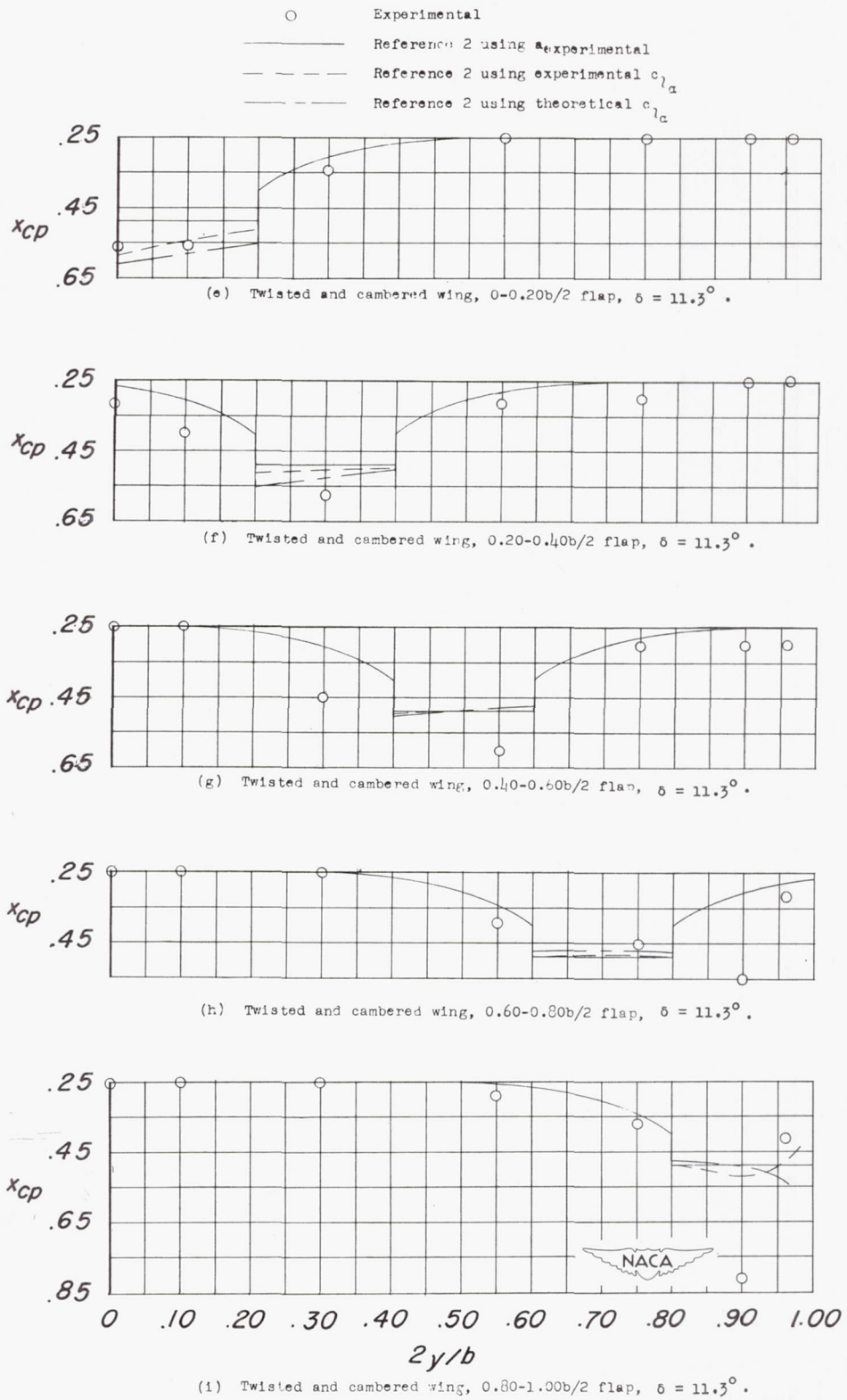


(e) Twisted and cambered wing, 0-0.20b/2 flap, $\delta = 11.3^\circ$.

(f) Twisted and cambered wing, 0.20-0.40b/2 flap, $\delta = 11.3^\circ$.

(g) Twisted and cambered wing, 0.40-0.60b/2 flap, $\delta = 11.3^\circ$.

(h) Twisted and cambered wing, 0.60-0.80b/2 flap, $\delta = 11.3^\circ$.

(i) Twisted and cambered wing, 0.80-1.00b/2 flap, $\delta = 11.3^\circ$.

Figure 10.- Concluded.